

Performance limitations of a free-space optical communication satellite network owing to vibrations: heterodyne detection

Shlomi Arnon, Stanley R. Rotman, and Norman S. Kopeika

Free-space optical communication between satellites in a distributed network can permit high data rates of communication between different places on Earth. To establish optical communication between any two satellites requires that the line of sight of their optics be aligned during the entire communication time. Because of the large distance between the satellites and the alignment accuracy required, the pointing from one satellite to another is complicated because of vibrations of the pointing system caused by two fundamental stochastic mechanisms: tracking noise created by the electro-optic tracker and vibrations derived from mechanical components. Vibration of the transmitter beam in the receiver plane causes a decrease in the received optical power. Vibrations of the receiver telescope relative to the received beam decrease the heterodyne mixing efficiency. These two factors increase the bit-error rate of a coherent detection network. We derive simple mathematical models of the network bit-error rate versus the system parameters and the transmitter and receiver vibration statistics. An example of a practical optical heterodyne free-space satellite optical communication network is presented. From this research it is clear that even low-amplitude vibration of the satellite-pointing systems dramatically decreases network performance. © 1998 Optical Society of America

OCIS codes: 060.0060, 060.4510, 040.2840, 120.7280, 200.2610.

1. Introduction

Global communication from any place on Earth is an attractive goal. One method to achieve this aim is to network satellites together to provide global coverage and access (Fig. 1). By this method the information is transferred from the ground to the nearest satellite above and relayed among satellites to the satellite above the destination. The last satellite then transmits the information to the destination. Optical intersatellite links have some advantages compared with microwave intersatellite links. The advantages of the optical intersatellite links are smaller size and weight of the terminal, less power consumption, greater immunity to interference, a larger data rate, and acceptability of denser satellite orbit population. The main disadvantage of optical intersatellite

links is the complexity of the pointing system, which derives from the necessity to point a narrow or slowly diverging laser beam from one satellite to another over a distance of tens of thousands of kilometers in the presence of relative motion and vibration. The pointing system compensates for the movement of the satellites by using the known Ephemerides data and signals from the electro-optic tracking system. The coupling of the satellite's mechanical vibration and tracking noise to the pointing system causes vibration of the satellite's transmitter beam in the receiver plane and the vibration of the satellite's receiver telescope relative to the received beam direction. Such vibrations decrease heterodyne mixing efficiency and the received optical power. These two phenomena increase the channel (receiver and transmitter satellite) bit-error rate (BER). In optical satellite networks the problem is more complicated because all the satellites continually vibrate randomly.

The concept of rf intersatellite link communication networks appears in the Iridium and Teledesic communications projects.^{1,2} The concept of optical intersatellite links in communication satellite networks appears in the Celestri multimedial system.³ References 4 and 5 review laser satellite communication

The authors are with the Department of Electrical and Computer Engineering, Ben-Gurion University of the Negev, P.O. Box 653, Beer-Sheva 84105, Israel. The email address for N. S. Kopeika is kopeika@bgu.ac.il.

Received 3 February 1998; revised manuscript received 8 May 1998.

0003-6935/98/276366-09\$15.00/0

© 1998 Optical Society of America

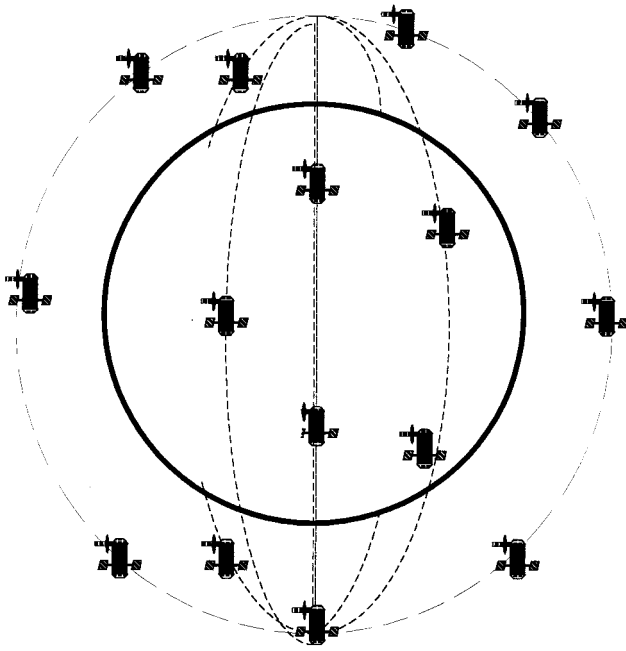


Fig. 1. Network of free-space optical communication satellites.

networks. Analysis of the performance of analog and digital direct-detection satellite optical communication networks is described in Refs. 6 and 7. Results of on-board measurements of satellite vibration spectra are specified in Ref. 8. Skormin *et al.* describe adaptive techniques to reduce effects of vibrations on the pointing system.⁹ Chen and Gardner¹⁰ analyze the effects of random pointing and tracking errors on the design of coherent and incoherent optical intersatellite communication links. Held and Barry,¹¹ using measured platform disturbance data, analyze the precision pointing and tracking accuracy that is possible between satellites. Barry and Mecherle¹² found relationships between the rms standard deviation of the pointing-error distribution and the burst error of the communication system. In Refs. 13–15 communication system solutions that are to tolerate vibrations are suggested. The book by Lambert and Casey¹⁶ describes most of the concepts of laser communication in space, including the effects of vibrations on the communication system.

Here we derive simple mathematical models of the network BER as a function of the network parameters and the transmitter and receiver vibration statistics. The uniqueness of our model is its capability to analyze most of the heterodyne detection scheme in one simple expression. An example of a practical optical heterodyne free-space satellite optical communication network is presented. From this research it is clear that even low-amplitude vibrations of the satellite-pointing systems dramatically decrease network performance. Our models can be the basis for satellite optical communication, tracking, and pointing-system design of appropriate complexity and performance to make the network as simple and inexpensive as possible.

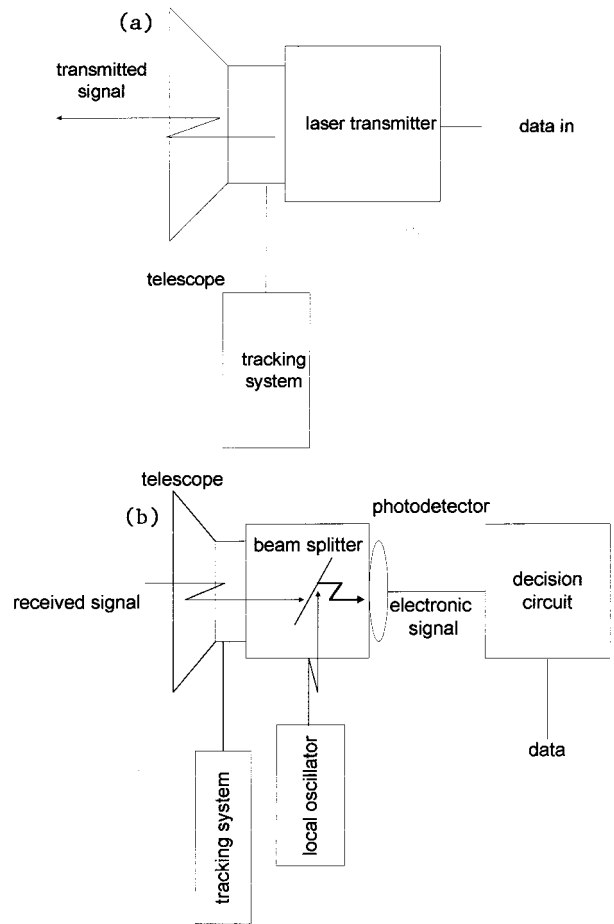


Fig. 2. Basic schematics of (a) a satellite heterodyne optical communication transmitter and (b) a satellite heterodyne optical communication receiver.

2. Satellite Heterodyne Detection Model

In this section we define the basic elements of the heterodyne transmitter and receiver in satellite optical communication networks. Figure 2 shows simple schematics of a heterodyne transmitter and receiver. The transmitter model includes a laser transmitter, a telescope, and a tracking system. The receiver model includes a telescope, a local oscillator (laser), a beam splitter, a detector, and a tracking system. The messages arrive at the input of the transmitter. The transmitter converts electrical signals into optical signals by using the laser. The transmitter telescope collimates the laser radiation in the receiver satellite direction, using data from the tracking system. The tracking system directs the receiver telescope in the direction of the transmitter satellite. Vibrations of receiver telescope direction in the receiver plane decrease the received optical power. The receiver telescope focuses the received radiation onto the detector. The radiation propagates through the beam splitter to the detector. The local-oscillator radiation is reflected by the beam splitter to the detector.

On the surface of the detector the heterodyne mixing of the received transmitter and local-oscillator

radiation is performed. Vibrations of the receiver telescope direction relative to the direction of the received radiation decrease the heterodyne mixing efficiency, which is extremely sensitive to alignment of the two beams. The detector converts the optical power into an electronic signal. The data are recovered from the electronic signal by a decision circuit.

3. Vibration Model

To establish optical communication between two satellites one must align the line of sight of their optics during the entire communication time. To meet this requirement satellites use the Ephemerides data (the position of the satellite according to the orbit equation) and navigation systems such as a star tracker or a global position system for rough pointing and a tracking system for fine pointing to the other satellite. The basic and popular method of tracking between satellites includes the use of a beacon signal and of a tracking system with a quadrant detector on each satellite of the communication channel. The tracking system works in direct-detection mode. In this section we present the statistics models of the receiver and transmitter pointing systems.

The fine elevation and azimuth angle of the pointing system use the output signal of the quadrant detector. Because of noise in the tracking system^{5,10} and mechanical vibrations^{5,8-10} the satellite's pointing direction vibrates. The orthogonal direction-error pointing-angle models of the vibrations are based on a normal distribution.¹⁰

The elevation-pointing-error angle is normally distributed with a probability density

$$f(\theta_v) = \frac{1}{\sqrt{2\pi}\sigma_v} \exp\left(-\frac{\theta_v^2}{2\sigma_v^2}\right), \quad (1)$$

where σ_v and θ_v are the elevation-pointing standard deviation and the elevation-pointing angle of a satellite (i) in the network, respectively.

The azimuth-pointing-error angle is normally distributed with a probability density

$$f(\theta_H) = \frac{1}{\sqrt{2\pi}\sigma_H} \exp\left(-\frac{\theta_H^2}{2\sigma_H^2}\right), \quad (2)$$

where σ_H and θ_H are the azimuth-pointing standard deviation and the azimuth-pointing angle of the satellite, respectively.

The radial-pointing-error angle is the root-square sum of the azimuth and elevation angles:

$$\theta = \sqrt{\theta_v^2 + \theta_H^2}. \quad (3)$$

Based on symmetry, we can assume that

$$\sigma_v = \sigma_H = \sigma. \quad (4)$$

We assume that the azimuth and elevation processes¹⁰ are independent and identically distributed so the radial-pointing-error angle model is Rayleigh distributed.

The probability-density function of the transmitter radial-pointing-error angle is

$$f_T(\theta_T) = \frac{\theta_T}{\sigma_T^2} \exp\left(-\frac{\theta_T^2}{2\sigma_T^2}\right). \quad (5)$$

The probability-density function of the receiver radial-pointing-error angle is

$$f_R(\theta_R) = \frac{\theta_R}{\sigma_R^2} \exp\left(-\frac{\theta_R^2}{2\sigma_R^2}\right). \quad (6)$$

4. Range Equation Model

In this section we derive a model that relates the optical power transmitted from the transmitter satellite to the optical power received by the receiver satellite. The distance between the transmitter and the receiver satellites (in meters) is z . The instantaneous received power as a function of pointing-direction-error angles θ_R and θ_T and the difference angle between the transmitter and the local-oscillator linear polarization θ_p is

$$P_R(\theta_T, \theta_R, \theta_p) = C_1 L_T(\theta_T) L_R(\theta_R) \cos^2(\theta_p), \quad (7)$$

where

$$C_1 = P_T \eta_R \eta_T G_R G_T [\lambda / (4\pi z)]^2 \quad (8)$$

and where η_R , η_T and G_R , G_T are the optical efficiencies and the telescope gain of the receiver and the transmitter, respectively. The wavelength of the laser transmitter is λ . P_T is the optical laser transmitter power, $L_T(\theta_T)$ is the transmitter pointing-loss factor, and $L_R(\theta_R)$ is the heterodyne pointing-loss factor.

The transmitted radiation pattern of a uniformly illuminated, diffraction-limited, unobscured circular aperture is given by $[2J_1(x)/x]^2$, where $J_1(x)$ is the Bessel function of the first order. For practical applications the intensity cross section of a single-mode laser can be better approximated by a Gaussian beam.¹⁵ This approach is used here.

The gain of the transmitter telescope is¹⁰

$$G_T = \left(\frac{2\pi W}{\lambda}\right)^2, \quad (9)$$

where W is the Gaussian rms width at the transmitter aperture. The transmitter pointing-loss factor is¹⁰

$$L_T(\theta_i) = \exp(-G_T \theta_i^2). \quad (10)$$

The heterodyne loss factor is¹⁷

$$L_R(q_0) = \left| \frac{1}{A} \int_{A_d} \phi_L(q) \phi_R^*(q - q_0) dq \right|^2, \quad (11)$$

where $\phi_R(q)$ is the diffraction pattern of the received field on the detector plane, $\phi_L(q)$ is the diffraction pattern of the local-oscillator field on the detector plane, A_d is the detector area, A is a normalization

factor, and q_0 is the offset distance from the detector center in the focal plane.

The transformation from offset at the detector plane to the receiver's radial-pointing-error angle is

$$\theta_R \approx q_0/f_0, \quad (12)$$

where f_0 is the receiver's focal length. From Eq. (11) and approximation (12) the heterodyne loss as a function of θ_R is

$$L_R(\theta_R) = \left| \frac{1}{A} \int_{A_d} \phi_L(q) \phi_R^*(q - \theta_R f_0) dq \right|^2. \quad (13)$$

The diffraction pattern of the received field $\phi_1(\theta_R)$ is caused primarily by diffraction with the receiver telescope's lens. It can be approximated by

$$\phi_R(q) = [2J_1(\sqrt{G_R q}/f_0)/(\sqrt{G_R q}/f_0)], \quad (14)$$

where the gain of the receiver telescope is

$$G_R = \left(\frac{\pi D_R}{\lambda} \right)^2 \quad (15)$$

and where D_R is the receiver's aperture diameter.

The diffraction pattern of the local-oscillator field $\phi_L(q)$ is determined by the receiver's design. Possible radiation patterns are uniform illumination if the laser light is defocused, $[2J_1(x)/x]$ if the laser light is focused by a lens, and a Gaussian pattern.

The value of the heterodyne loss [Eq. (13)] depends on the radiation patterns of the received and the local-oscillator fields, the detector area, and the misalignment between the two fields. The approximation to the heterodyne loss, which was derived by Chen and Gardner,¹⁰ is

$$L_R(\theta_R) = [2J_1(\sqrt{G_R \theta_R})/(\sqrt{G_R \theta_R})]^2. \quad (16)$$

A more complex and accurate expression but without closed form for the heterodyne loss is presented by Gagliardi and Karp.¹⁷

5. Signal-to-Noise Ratio

In this section we define the basic models of signal and noise. We use them in the next sections to build complex models of system performance for various modulation schemes. Our receiver includes a p-i-n photodiode. This photodiode converts optical power into an electronic signal.

The responsivity of the p-i-n is¹⁸

$$R = \frac{q_e \eta}{h\nu}, \quad (17)$$

where q_e is the electron charge, η is the quantum efficiency, ν is the optical radiation frequency, and h is Planck's constant.

The instantaneous signal (the received square current) as a function of angles θ_p , θ_R , and θ_T is

$$S(\theta_T, \theta_R, \theta_p) = 4R^2 P_R(\theta_T, \theta_R, \theta_p) P_{LO}, \quad (18)$$

Table 1. Parameters K_1 and K_2 for Detection Schemes^a

Modulation Scheme ^b	K_1	K_2
Heterodyne asynchronous detection		
ASK envelope	0.5	0.25
FSK dual-filter	0.5	0.5
FSK single-filter	0.5	0.25
CPFSK	0.5	1
DPSK	0.5	1
Heterodyne synchronous detection		
PSK	1	1
FSK	1	0.5
ASK	1	0.5
Homodyne detection		
PSK	1	2
ASK	1	1
FSK	1	0.5

^aFrom Refs. 18 and 19.

^bASK, amplitude-shift keying; FSK, frequency-shift keying; CPFSK, continuous phase FSK; DPSK, differential phase shift keying.

where P_{LO} is the local-oscillator power. In our analysis we assume that the local-oscillator shot noise is the dominant noise source. The local-oscillator shot noise is given by¹⁸

$$N = 2qRP_{LO}B_W, \quad (19)$$

where B_W is the communication system's electronic bandwidth.

From Eqs. (7), (18), and (19) the instantaneous signal-to-noise ratio as a function of angles θ_p , θ_R , and θ_T is

$$\begin{aligned} \text{SNR}(\theta_T, \theta_R, \theta_p) &= \frac{S(\theta_T, \theta_R, \theta_p)}{N} \\ &= \frac{2RC_1 L_T(\theta_T) L_R(\theta_R) \cos^2(\theta_p)}{qB_W}. \end{aligned} \quad (20)$$

6. Channel Bit-Error-Rate Model

In this section we derive the channel BER that includes two satellites: a transmitter and a receiver. For most of the detection schemes we can approximate the BER by the exponential expression^{18,19}

$$\text{BER} = K_1 \exp(-K_2 \text{SNR}). \quad (21)$$

The parameters K_1 and K_2 for different detection schemes are listed in Table 1.

When some of the system parameters are random variables the instantaneous BER is given by

$$\text{BER}(\theta_T, \theta_R, \theta_p) = K_1 \exp[-K_2 \text{SNR}(\theta_T, \theta_R, \theta_p)]. \quad (22)$$

The average BER is defined by

$$\begin{aligned} \text{BER} = & \int_0^\infty \int_0^\infty \int_0^\infty K_1 \exp[-K_2 K_3 \exp(-G_T \theta_T^2) L_R(\theta_R)] \\ & \times \cos^2(\theta_p) \frac{\theta_T}{\sigma_T^2} \exp\left(-\frac{\theta_T^2}{2\sigma_T^2}\right) \frac{\theta_R}{\sigma_R^2} \\ & \times \exp\left(-\frac{\theta_R^2}{2\sigma_R^2}\right) f_p(\theta_p) d\theta_p d\theta_T d\theta_R, \end{aligned} \quad (23)$$

where $f_p(\theta_p)$ is the polarization angle's density-distribution function.

From Eqs. (7), (8) and (20),

$$K_3 = 2RP_T \eta_R \eta_T G_R G_T [\lambda / (4\pi z)]^2 / (qB_W). \quad (24)$$

Using the heterodyne loss [Eq. (16)] in Eq. (23) yields

$$\begin{aligned} \text{BER} = & \int_0^\infty \int_0^\infty \int_0^\infty K_1 \exp\left\{-K_2 K_3 \exp(-G_T \theta_T^2)\right. \\ & \times \left.\left[\frac{2J_1(\sqrt{G_R} \theta_R)}{(\sqrt{G_R} \theta_R)}\right]^2 \cos^2(\theta_p)\right\} \frac{\theta_T}{\sigma_T^2} \exp\left(-\frac{\theta_T^2}{2\sigma_T^2}\right) \frac{\theta_R}{\sigma_R^2} \\ & \times \exp\left(-\frac{\theta_R^2}{2\sigma_R^2}\right) f_p(\theta_p) d\theta_p d\theta_T d\theta_R. \end{aligned} \quad (25)$$

We assume that the polarization is not changing or is changing slowly, so the receiver adapts its local-oscillator polarization perfectly to those changes. Based on this assumption, Eq. (25) becomes

$$\begin{aligned} \text{BER} = & \int_0^\infty \int_0^\infty K_1 \exp\left\{-K_2 K_3 \exp(-G_T \theta_T^2)\right. \\ & \times \left.\left[\frac{2J_1(\sqrt{G_R} \theta_R)}{(\sqrt{G_R} \theta_R)}\right]^2\right\} \frac{\theta_T}{\sigma_T^2} \exp\left(-\frac{\theta_T^2}{2\sigma_T^2}\right) \frac{\theta_R}{\sigma_R^2} \\ & \times \exp\left(-\frac{\theta_R^2}{2\sigma_R^2}\right) d\theta_T d\theta_R. \end{aligned} \quad (26)$$

We define two new variables:

$$T = \theta_T / \sigma_T, \quad (27)$$

$$R = \theta_R / \sigma_R. \quad (28)$$

From Eqs. (26)–(28),

$$\begin{aligned} \text{BER} = & \int_0^\infty \int_0^\infty K_1 \exp\left\{-K_2 K_3 \exp(-G_T \sigma_T^2 T^2)\right. \\ & \times \left.\left[\frac{2J_1(\sqrt{G_R} R \sigma_R)}{(\sqrt{G_R} R \sigma_R)}\right]^2 - \frac{T^2 + R^2}{2}\right\} TR dR dT. \end{aligned} \quad (29)$$

In the following equations we simplify Eq. (29) to get a closed and simple expression for the BER. We approximate Eq. (16) by

$$L_R(\theta_R) \approx \exp(-G_T \theta_R^2). \quad (30)$$

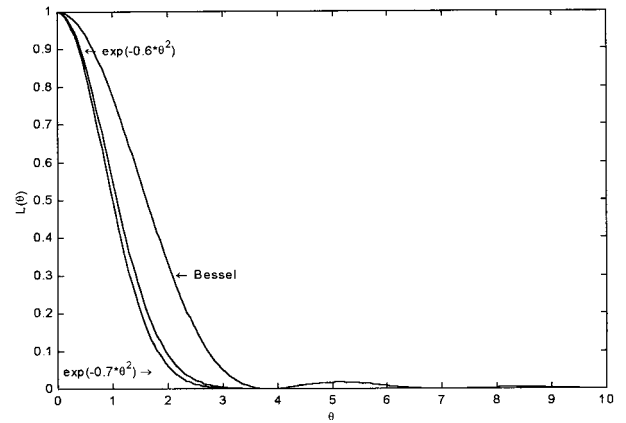


Fig. 3. Loss pattern as a function of misalignment angle.

All the satellites in the network are identical and use the same telescope for transmitting and receiving, such that

$$D_R = D_T. \quad (31)$$

Based on Eqs. (9), (10), and (31), width W of the transmitter beam at the transmitter aperture is less than the radius of the transmitter aperture:

$$D_R > 2W. \quad (32)$$

Figure 3 shows the loss patterns for $[2J_1(\theta)/(\theta)]^2$, $\exp(-0.6\theta^2)$, and $\exp(-0.7\theta^2)$ as a function of θ . From Fig. 3 and Appendix A it can be seen that the patterns are very similar and that an exponential expression is good approximation to $L_R(\theta_R)$ over a large range of practical values between D_R and W .

From Eq. (29) and relation (30),

$$\begin{aligned} \text{BER} = & \int_0^\infty \int_0^\infty K_1 \exp\left[-K_2 K_3 \exp(-G_T \sigma_T^2 T^2)\right. \\ & \times \left.\exp(-G_T \sigma_R^2 R^2) - \frac{T^2 + R^2}{2}\right] TR dR dT. \end{aligned} \quad (33)$$

The performances of the satellites' tracking and pointing systems are identical, so

$$\sigma_T \approx \sigma_R. \quad (34)$$

From Eq. (33) and relation (34),

$$\begin{aligned} \text{BER} = & \int_0^\infty \int_0^\infty K_1 \exp\left\{-K_2 K_3 \exp[-G_T \sigma_T^2 (T^2 + R^2)]\right. \\ & \times \left.\left[\frac{T^2 + R^2}{2}\right]\right\} TR dR dT. \end{aligned} \quad (35)$$

We define a new random variable:

$$y = T^2 + R^2. \quad (36)$$

We can also write y as the sum of the azimuth and elevation processes, which are independent and identically distributed. From Eqs. (3) and (36),

$$y = R_{RV}^2 + T_{TV}^2 + R_{RH}^2 + T_{TH}^2. \quad (37)$$

Because R_{RV} , T_{TV} , R_{RH} , and T_{TH} are normal independent, identically distributed random variables, y is distributed chi-square with four degrees of freedom. The density-distribution function of y is

$$f(y) = C_2 y^{-1+n/2} \exp[-y/(2\sigma_T^2)], \quad y \geq 0, \quad (38)$$

where

$$C_2 = [(\sqrt{2})^n \Gamma(n/2)]^{-1}, \quad (39)$$

$$n = 4. \quad (40)$$

From Eqs. (39) and (40),

$$C_2 = 1/(4\sigma_T^4). \quad (41)$$

From Eqs. (38) and (41), the density-distribution function of y is given by

$$f(y) = y/4 \exp(-y/2), \quad y \geq 0. \quad (42)$$

From Eqs. (35) and (42),

$$\text{BER} = \int_0^\infty K_1 \exp\left[-a \exp(-G_T \sigma_T^2 y) - \frac{y}{2}\right] \frac{y}{4} dy, \quad (43)$$

where the normalized signal-to-noise ratio is

$$a = K_2 K_3. \quad (44)$$

We simplify Eq. (35) from two integral equations to only one, which is Eq. (43). Next we express Eq. (43) in a more compact and simple form. We define a new variable such that

$$Z = \exp(-y/2). \quad (45)$$

From Eqs. (43) and (45), the simplest form of the channel BER is given by

$$\text{BER}_{\text{channel}} = \text{BER} = -K_1 \int_0^1 \ln(Z) \exp(-Z^b a) dZ, \quad (46)$$

where

$$b = 2G_T \sigma_\theta^2. \quad (47)$$

For efficient numerical calculation of Eq. (46) we use Eqs. (B1)–(B3) from Appendix B. Equation (46) describes the BER of an optical intersatellite link as a function of three parameters: normalized signal-to-noise ratio a [Eqs. (44) and (24)], the normalized vibration amplitude b [Eq. (47)], and modulation constant K_1 from Table 1. From Eq. (47) we can see that increase of the normalized signal-to-noise ratio a decreases the exponent in Eq. (46) and yields a lower BER. On the other hand, increase of the normalized vibration b decreases the Z^b expression, increases the exponent, and yields a higher BER. The effect of modulation parameter K_1 on the BER is minor (it

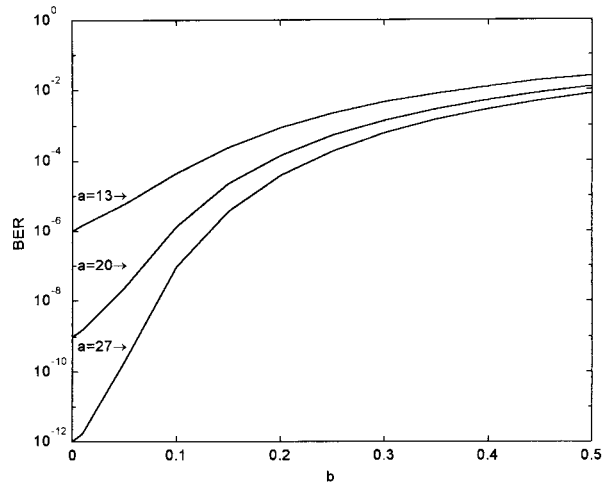


Fig. 4. Channel BER as a function of normalized vibration amplitude b . $K_1 = 0.5$.

takes the value 0.5 or 1). Figure 4 shows the channel BER for K_1 equal to 0.5 and a equal to 13, 20, and 27, versus the normalized vibration amplitude b . From this figure it is easy to see the dramatic effect of the vibration on the BER no matter what channel margin we have.

7. Network Bit Error Rate

In this section we derive a model to describe the performances of satellite optical communication networks. This model is only for the intersatellite link. The performances of the optical and the rf up and down links are beyond the scope of this analysis. In this network the message is transferred from the satellite above the ground source, between successive network satellites and, finally, to the satellite above the ground destination. The message is passed through n satellites. The result of this model is the BER of the network for a message passing through n satellites.

The BER of a satellite communication network with n satellites is

$$\text{BER}_{\text{network}} \approx 1 - \prod_{i=1}^n [1 - \text{BER}_{\text{channel}}(i)]. \quad (48)$$

If the BER is very small, i.e.,

$$\text{BER}_{\text{channel}}(i) \ll 1, \quad \forall i, \quad (49)$$

we can neglect all channel BER's with exponents greater than unity, so inequality (49) simplifies to

$$\text{BER}_{\text{network}} \approx \sum_{i=1}^n [\text{BER}_{\text{channel}}(i)]. \quad (50)$$

We simplify relation (50) for two extreme cases.

In case (I) all the satellites are identical. If

$$\text{BER}_{\text{network}}(i) = \text{BER}_{\text{channel}}(j), \quad \forall i, j, \quad (51)$$

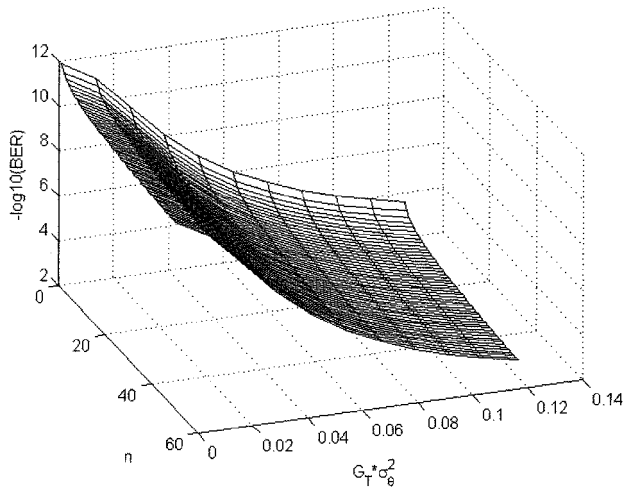


Fig. 5. Network BER as a function of normalized vibration amplitude and the number of satellites in the network.

relation (50) simplifies to

$$\text{BER}_{\text{network}} \approx n \text{BER}_{\text{channel}(1)}. \quad (52)$$

In case (II) one satellite has a higher BER because of vibration. If

$$\text{BER}_{\text{channel}(i)} \gg \text{BER}_{\text{channel}(j)}, \quad \forall j, \quad (53)$$

relation (50) simplifies to

$$\text{BER}_{\text{network}} \approx \text{BER}_{\text{channel}(i)}. \quad (54)$$

From relation (54) it is seen that one satellite can determine the performance of the entire network.

Figure 5 describes the network BER as a function of normalized vibration amplitude b and the number of satellites in the network according to relation (50). Figure 5 shows that the BER increases as the vibration variance and the number of satellites in the network increase. From this figure we can see that the vibration amplitude is the dominant performance parameter and that the size of the network is a minor performance parameter. The conclusion in relation (54) that the performance of the network is determined by the satellite in the network that vibrates most can be seen easily from Fig. 5.

8. Example of a Practical Communication System

The situation considered here is that of a communication network link between ten low-Earth-orbit (LEO) satellites (similar to the Celestri multimediam system³). The network includes a transmitter satellite above ground or an airborne transmitter, regenerative satellites, and a receiver satellite above ground or an airborne receiver. The information is received in a transmitter satellite from a rf ground or air station. This information is then upconverted into an optical signal and transmitted to the neighboring regenerative satellite. The information is passed between the regenerative satellites to the receiver satellite. At the receiver satellite the information is downconverted into rf and transmitted to a

Table 2. Parameters of a Practical Optical Communication Satellite Network

Parameter Name	Parameter Symbol	Parameter Value
Optical wavelength	λ	0.8 μm
p-i-n Quantum efficiency	η	0.8
Transmitter power	P_T	1 W
Gaussian rms width	W	0.01435 m
Receiver optics efficiency	η_R	0.8
Transmitter optics efficiency	η_T	0.8
Distance between satellites	z	5000 km
Bit-rate electronic bandwidth	B_W	2 Gbits/s
Network size	N	10

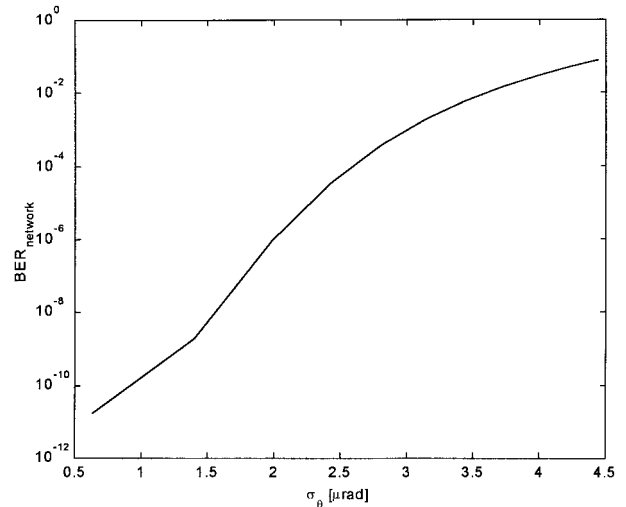


Fig. 6. Network BER versus vibration amplitude.

ground or an air station. The satellites are placed at an orbit altitude of ~ 1400 km. The distance between the neighboring satellites is assumed to be 5000 km. The communication system uses a frequency-shift-keying heterodyne asynchronous detection mode. The important parameters of the communication systems are the following: the bit rate is 2 Gbits/s, the optical wavelength is 0.8 μm , and the transmitter power is 1 W. All the other parameters are listed in Table 2. Considering these data, we examine the effect of the vibration on the performance of the network, using relation (52). In Fig. 6 we can see the network BER versus the vibration amplitude. The network BER changes from an 10^{-11} to an $\sim 10^{-1}$ change in vibration amplitude from 0.5 to 4.5 μrad . From this Figure it can be seen that the network BER decreases rapidly in response to a small change in the vibration variance. This analysis points out that even low-value vibration amplitudes in each satellite can dramatically decrease the performance of the network.

9. Summary and Conclusions

We have studied the effects of vibrations of the pointing system on the performance of optical communication satellite heterodyne networks. The analysis

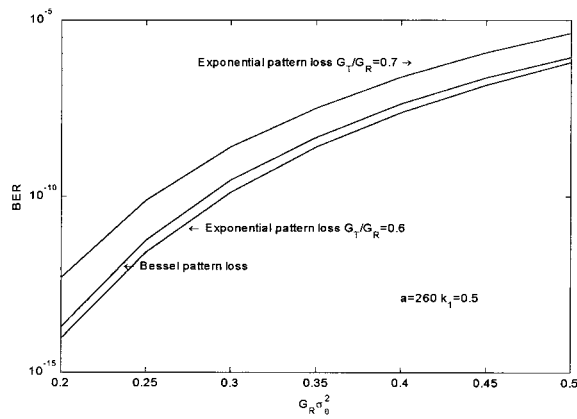


Fig. 7. BER as a function of $G_R\sigma_0^2$.

carried out here can be the basis for future analyses of optical communication networks. This analysis pointed out that even low values of vibration amplitudes in each satellite can dramatically decrease the performance of that network. The vibration amplitude is the dominant network performance parameter, and the size of the network is a minor network performance parameter. One important conclusion is that the performance of the network is determined by the satellite that vibrates the most among the satellites in the network. This research is a continuation of our previous research on analog and digital optical satellite communication networks.^{5,6}

Appendix A

We compare the BER's of optical links with exponential and Bessel pattern heterodyne mixing losses. Figure 7 shows the BER for Bessel and exponential pattern losses versus $G_R\sigma_0^2$. The BER curve with Bessel heterodyne mixing loss is bounded above and below by BER curves with $\exp(-0.7G_R\sigma_0^2)$ and $\exp(-0.6G_R\sigma_0^2)$ heterodyne mixing losses, respectively. From Fig. 7 it is easy to see that the exponential function yields similar results to the Bessel function for calculation of the BER. The ratio $2W/D_R$ yields 0.85 and 0.76, respectively, leading to the factors $0.7G_R$ and $0.6G_R$ in the exponential. The Gaussian rms width at the transmitter aperture W is smaller than the aperture radius to prevent diffraction, so the ratios 0.85 and 0.76 are practical engineering values. In this appendix we have shown that the exponential function is a good approximation for the Bessel function for a wide range of vibration amplitudes.

Appendix B

The numerical calculation of Eq. (B1) is more efficient if we substitute Eq. (B2). The result of the substitution is Eq. (B3):

$$c = - \int_0^1 \ln(z) \exp(-az^b) dz. \quad (\text{B1})$$

We substitute t for Z^b :

$$t = Z^b. \quad (\text{B2})$$

From Eqs. (B1) and (B2),

$$c = - \frac{1}{b^2} \int_0^1 \ln(t) \exp(-at) t^{(1/b)-1} dt. \quad (\text{B3})$$

The authors are grateful for the help of Mark Auslander of the Department of Electrical and Computer Engineering, Ben Gurion University of the Negev, and for the support of the Ministry of Science and Technology, Jerusalem, Israel, for Shlomi Arnon.

References

1. R. J. Leopold and A. Miller, "The Iridium communications system," *IEEE Potential* **12**(2), 6–9 (1993).
2. P. P. Giusto and G. Quaglione, "Technical alternative for satellite mobile network," in *Mobile and Personal Satellite Communications, Proceedings of the First European Workshop on Mobile/Personal Satcoms*, F. Ananasso and F. Vatalaro, eds., (Springer-Verlag, Berlin, 1995), pp. 15–27.
3. Motorola Global Communication, "Application for Celestri multimedia LEO system," (Federal Communication Commission, Washington, D.C., 1997), p. 41.
4. B. I. Edelson and G. Hyde, "Laser satellite communications, program technology and applications," a report of the IEEE–USA Aerospace Policy Committee (IEEE, Piscataway, N.J., 1996).
5. S. Arnon and N. S. Kopeika, "Laser satellite communication networks—vibration effects and possible solutions," *Proc. IEEE* **85**, 1646–1661 (1997).
6. S. Arnon and N. S. Kopeika, "The performance limitations of free space optical communication satellite networks due to vibrations— analog case," *Opt. Eng.* **36**, 175–182 (1997).
7. S. Arnon, S. Rotman, and N. S. Kopeika, "The performance limitations of free space optical communication satellite networks due to vibrations—digital case," *Opt. Eng.* **36**, 3148–3157 (1997).
8. M. Wittig, L. van Holtz, D. E. L. Tunbridge, and H. C. Vermeulen, "In orbit measurements of microaccelerations of ESA's communication satellite OLYMPUS," in *Selected Papers on Free-Space Laser Communication II*, D. L. Begly and B. J. Thompson, eds. Vol. 100 of SPIE Milestone Series (SPIE, Bellingham, Wash., 1994), pp. 389–398.
9. V. A. Skormin, M. A. Tascillo, and T. E. Busch, "Adaptive jitter rejection technique applicable to airborne laser communication systems," *Opt. Eng.* **34**, 1263–1268 (1995).
10. C. C. Chen and C. S. Gardner, "Impact of random pointing and tracking errors on the design of coherent and incoherent optical intersatellite communication links," *IEEE Trans. Commun.* **37**, 252–260 (1989).
11. K. J. Held and J. D. Barry, "Precision pointing and tracking between satellite-borne optical systems," *Opt. Eng.* **27**, 325–333 (1988).
12. J. D. Barry and G. S. Mecherle, "Beam pointing error as a significant parameter for satellite borne, free-space optical communication systems," *Opt. Eng.* **24**, 1049–1054 (1985).
13. S. Arnon, S. Rotman, and N. S. Kopeika, "Beam width and transmitter power adaptive to tracking system performance for free-space optical communication," *Appl. Opt.* **36**, 6095–6101 (1997).
14. S. Arnon, S. Rotman and N. S. Kopeika, "Optimum transmitter

- optics aperture for satellite optical communication," IEEE Trans. Aerosp. Electron. Syst. (to be published).
15. S. Arnon and N. S. Kopeika, "Adaptive bandwidth for satellite optical communication," IEE Proc. Optoelectron. **145**(2) (April 1998).
 16. S. G. Lambert and W. L. Casey, *Laser Communication in Space* (Artech, Boston, Mass., 1995).
 17. R. M. Gagliardi and S. Karp, *Optical Communication*, 2nd ed. (Wiley, New York, 1995), pp. 32–34, 201–206, 247.
 18. L. Kazovsky, S. Benedetto, and A. Willner, *Optical fiber Communication Systems* (Artech, Boston, Mass., 1996), pp. 78–79, 248, 401–426.
 19. S. Ryu, *Coherent Lightwave Communication System* (Artech, Boston, Mass., 1994), pp. 41–65.